

INVESTIGATION ON USE OF PLUG-IN HYBRID ELECTRIC VEHICLE (PHEV) TECHNOLOGY USING RENEWABLE ENERGY FOR AN AUTORICKSHAW

Vishnu Padmanaban, Ajaykrishna Ramasubramanian, Thirumalini Subramaniam

*Amrita Vishwa Vidyapeetham (University)
Department of Mechanical Engineering
Amrita Nagar 641112, Coimbatore, India
tel.: +91 8098953570, +91 944251765, +91 9442018338
e-mail: vishnu1692@gmail.com
ajaykrishna2404@gmail.com, st_malini@cb.amrita.edu*

Abstract

Availability and access to energy are considered as catalysts for economic growth. Harnessing clean energy for sustainable development is the keyword in today's scenario of energy utility. With the transport sector, contributing 32% of the total pollution levels, development and increased utilization of hybrid electric vehicles would be the best possible method to adopt for a cleaner and greener tomorrow. While lithium-ion technology is expected in production HEVs in the very near future, use in PHEVs are expected to be more gradual and dependent on solving the life, safety, and cost challenges. As a result, battery technologies for EVs are not fully matured due to range and charging-time issues, which are yet to be addressed. These two issues are normalized substantially in our study as the result of implementation of a battery swapping technique, thereby fast charging the batteries. This study focuses on battery systems as the electrical energy storage device and thus evaluates commercially available technologies for PHEV penetration in India through use of renewable energy sources such as wind and solar power in specific demographic areas as a typical example. The three-wheeler vehicle, popularly known as auto-rickshaws are one of the most important type of commercial transportation in majority of the Indian cities. An example of such a typical urban use auto rickshaw is considered for our study. This project has three main objectives: To convert the existing three wheeler into a PHEV and to determine the state of technology for PHEV batteries through an extensive literature review, develop a battery pack model and its charging cum swapping station at the above two places using renewable energy sources and finally to assess the environmental benefits of greenhouse gases emission, CO₂ reduction and decrease in fuel consumption.

Keywords: PHEV, renewable energy, smart grid, vehicle to grid, fast charging, auto rickshaw

1. Introduction

India is in a position to be counted as one of the emerging economies of the world with the automobile sector, responsible for nearly 18% of the carbon di-oxide emissions. Electricity demand has created a peak energy shortage of around 12.7%. To meet this shortfall, the cleanest available option to India is Renewable Energy Technology (RET) which is poised to play a crucial role in India's emerging energy requirement. The very need to harness wind energy to power the PHEVs lies in the fact that with the present level of momentum established in India's wind sector, the ten years between 2020 and 2030 could see spectacular growth if some of the systemic barriers are addressed in a timely manner. The reason for choosing the three-wheel auto rickshaw for our study is that, these vehicles encourage the use of public transport. Also, it is the most preferred means of transport as compared to personal modes of transport by a majority of people in the urban and sub-urban parts of the country. Greater usage of such vehicles reduces parking problems and emits less pollution, than with that of the usage of less than 1000 cc cars.

Harnessing solar energy has a huge potential in India due to its geographic location. PHEV technology presents an excellent way to reduce petroleum consumption and reduction in

environmental pollution rates through efficient improvements such as fuel flexibility, extended range for long-range commuters and availability of charging stations to ease re-fuelling of the vehicle, thus providing a smart and sustainable mobility. This paper provides a synergy between the PHEVs and the renewable energy with an investigation on battery modelling. A discussion on the charging station infrastructure equipped with battery swap technique is also made. Equipping PHEVs with the bi-directional connection to the electric grid offers new opportunities for both transportation and power generation sectors. A typical example of Coimbatore, a tier two city with about 2000 auto rickshaws plying within the city limits with an average trip distance of around 40km is considered for the study.

2. Energy Storage System (ESS)

The researchers have long viewed lithium batteries as an attractive alternative to the expensive metal-based batteries, which have been used in the recent past for the hybrid/battery electric vehicles. Considering the various possible types and its commerciality, there are four suitable types available for PHEV operation viz., LiFePO₄ (LFP), LiNiMnCoO₂ (NMC), LiMn₂O₄ (Mn-spinel) and LiNiCoAlO₂ (NCA). On comparing the technical aspects among these different batteries (Tab. 1), it is found that the li-ion manganese based chemistry has the required parameters such as chemical stability, abuse tolerance, high power performance, fast charging capability, good cycle life and calendar life, which are critical for a PHEV operation. However, the challenges of manganese based battery type such as cycle life problems due to manganese dissolution and low energy capacity are possibly made to overcome by using a mixture of spinel and nickelate to improve the cycle life characteristics and enhancing the energy capacity of the battery system. Li-manganese has a capacity that is roughly one-third lower compared to Li-cobalt but the battery still offers about 50 percent more energy than nickel-based chemistries [1]. The possible difficulties with the use of Mn-Spinel chemistry is that the specific energy is almost half that of the other battery types. In this case using a cathode combination of one-third nickel, one-third manganese and one-third cobalt offers a unique blend for Li-NMC that also lowers raw material cost due to reduced cobalt content. NMC has good overall performance and excels on specific energy. This battery is the preferred candidate for our electric vehicle and has the lowest self-heating rate. Although the power density of cobalt based batteries are high, the safety parameter is reasonably good in manganese based li-ion systems. In choosing the optimum power density, there is usually an inevitable trade-off in energy density, which should be considered, so as to account for the requirements of the pulse power characteristics of the vehicle.

Tab. 1. Comparison characteristics of li-ion battery candidates [2]

| Parameter | Unit | NCA- graphite | LFP-graphite | NMC-graphite | MNS |
|-----------------------------|-----------------|---------------|--------------|--------------|------------|
| Cell capacity | Ah | 2.7 | 0.45 | 2.8 | 3.6 |
| Max. Voltage on charging | V | 4.2 | 3.8 | 4.2 | 4.2 |
| Avg. Voltage on discharge | V | 3 | 3.2 | 3.7 | 3.75 |
| Operating temperature | °C | ~ -30°C/60°C | ~ -20°C/60°C | -40°C/60°C | -20°C/55°C |
| Total cell area | cm ² | 12.11 | 8.76 | 11.86 | 12.56 |
| Cell weight | g | 45 | 16.5 | 46 | 300 |
| Cell – specific power | W/kg | 770 | 1600 | 650 | 2000 |
| Cell – specific energy | Wh/kg | 101-108 | 74-94 | 125-150 | 54 |
| Safety | | Moderate | Excellent | Good | Poor |
| Economy | | Poor | Excellent | Good | Moderate |
| Cold. Temperature Operation | | Poor | Excellent | Good | Moderate |

2.1. Thermal Management of ESS

Thermal management of batteries is essential for high power applications as in traction batteries, where the safety from thermal hazards and improvement in cycle life is necessary. Passive thermal management system, which eliminates the use of large active cooling systems, is gaining wide popularity among the lightweight and low power hybrid electric vehicle development. This type of system involves the use of phase change material (PCM), which acts as a heat sink absorbing all the heat, which is dissipated by the battery system. The battery cells are embedded in a matrix of graphite, which holds the cells along with the PCM materials in direct contact. The materials are generally classified into three types as salt hydrates, eutectics and organic materials, depending upon the intensity of the heat absorption required for the battery system. Paraffin wax, a type of organic PCM is usually encapsulated in the graphite matrix to produce a composite with high thermal conductivity and high latent heat storage. The increase in thermal conductivity in the PCM absorbs and releases heat from the cell efficiently. The requirements of Thermal Management System (TMS) of an auto rickshaw are determined (Tab. 2). Comparing the requirements of the TMS of our vehicle taken for study and the properties of the different PCM candidates, it is clearly evident that the use of paraffin wax material as the PCM is desirable for our application. Thus, the use of PCM for the battery pack eliminates the disadvantages of air cooling system such as cell temperatures reaching above the safety limit, thereby maintaining the battery capacity. Also, the battery pack does not require fan power as in case of active cooling and thus, the cell temperature in the pack is maintained uniform. The selection criteria of a PCM from the different candidates available, is influenced broadly by four factors namely thermodynamic properties, kinetic properties, chemical properties and economic factors. The rate of heat generation is given by the sum of heat generated due to temperature change and heat generated due to increase in internal resistance of the cell. All the types of lithium ion battery have a temperature rise of up to 80°C from the room temperature under high discharge rates of PHEV operation. But the operating temperature of the vehicle is always maintained below 45°C. Therefore the heat generated after 45°C was taken up by the passive PCM systems which is calculated with equation (1)

$$H = mC_p \Delta T + i^2 R T_f, \quad (1)$$

where:

- H – total heat generated by each cell of the battery pack (kJ),
- m – mass of the material of the cell (kg),
- C_p – specific heat at constant pressure ($\text{J kg}^{-1} \text{K}^{-1}$),
- ΔT – change in temperature (K),
- i – discharge current (A),
- R – internal resistance of the battery (K),
- T_f – final temperature of the battery (K).

Tab. 2. Total heat generated by a single cell of the traction battery pack

| LITHIUM BATTERY TYPE | INTERNAL RESISTANCE (m ohm) | SPECIFIC HEAT CAPACITY (J/kg K) | CURRENT (I) | HEAT GENERATED (J) | TOTAL HEAT GENERATION (kJ) |
|----------------------|-----------------------------|---------------------------------|-------------|--------------------|----------------------------|
| LFP | 1 | 955.4 | 0.45 | 551.74 +0.729 | 0.552 |
| NMC | 1.1 | 795 | 2.8 | 1279.95+3.1046 | 1.283 |

Based on the heat generation data of the battery system, the volume of the PCM required is calculated as given in equation (2).

$$V = \frac{Q t}{\rho [L + C_p (T_m - T_0)]}, \quad (2)$$

where:

V – volume of the PCM material required (m^3),

Q – heat generated by the battery pack (kJ),

t – time (s),

ρ – density (kg/m^3),

L – half of slab thickness (m),

C_p – specific heat at constant pressure,

T_m – final temperature (K)

T_0 – initial temperature (K)

This volume of PCM can be used either to calculate the PCM mass or, the thickness by dividing V_{PCM} by the surface area. Thus, the mass quantity of PCM required is determined to be 12 g/cell corresponding to the chosen paraffin wax material.

Tab. 3. Properties comparison of different PCM material candidates [3]

| Property | Organic Paraffin | Organic Non-Paraffin | Inorganic Salt Hydrate | Inorganic Metal Eutectic |
|---|------------------|--------------------------------|--------------------------------------|--------------------------|
| $h_v(\text{kJ/kg})$ | 230- 290 | 120- 240 | 170- 340 | 30- 90 |
| $h_fv([\text{J}/\text{m}^3] \times 10^6)$ | 190- 240 | 140- 430 | 250-660 | 300-800 |
| Density (kg/m^3) | ~810 | 900-1800 | 900-2200 | ~8000 |
| $k (\text{W}/\text{m}^\circ\text{C})$ | ~0.25 | ~0.2 | 0.6-1.2 | ~20 |
| Heat Conductivity | High | Moderate | High | Low |
| Congruent melt | Yes | Some Do | Most Do Not | Yes |
| Super cool | No | No | Most Do | No |
| Stability | Good | Very low at higher temperature | Additives improves cycling stability | Moderate |

3. Power and Energy requirements

Auto rickshaw- the vehicle chosen for study is, as shown in Fig. 2 and its vehicle parameters and the performance requirements are depicted in the Tab. 4 and Tab. 5 respectively.



Fig. 1. Vehicle chosen for study

Tab. 4. Vehicle parameters

| | |
|-------------------------|---------------------|
| Kerb weight | 272 kg |
| Gross vehicle weight | 610 kg |
| Frontal area | 2.0 m ² |
| Coefficient of drag | 0.44 |
| Wheel radius | 0.4064 m |
| Tire rolling resistance | 0.015 |
| Gear ratios | 5, 2.93, 1.84, 1.12 |
| Final drive ratio | 4.125 |

Tab. 5. Performance characteristics of vehicle

| Parameter | Unit | Value |
|---------------|------|---------------|
| 0-60 kmph | s | 19.6 |
| 0-30kmph | s | 6.6 |
| Grade at kmph | % | 12% at 10kmph |
| Maximum speed | kmph | 50 |

From the requirements stated in Tab. 3, the vehicle traction losses and the corresponding tractive power is calculated. This power is compared with the value obtained from the road load power to check if the power requirement would suffice. The driving cycle pattern of the urban condition is as shown in Fig. 2 and Fig. 3. Thus, from the graph it is evident that the power requirement of the vehicle, considering the worst condition of the aggressiveness of the driver is within the limits of the power capability of the vehicle. Also, the energy consumption of the vehicle is within the estimated energy usage of 105Wh/km.

Tab. 6. Tractive losses of the vehicle

| Power Loss/Gain type | Unit | Value |
|-------------------------|------|--------|
| Aerodynamic drag loss | N | 82.5 |
| Rolling resistance loss | N | 89.761 |
| Road inclination loss | N | 72.875 |

The continuous power rating of the motor is sized to this value of 15 kW and the size of the auxiliary power unit is determined to be 3.8 kW. Based on the average power duration and the idling time of the modified Indian driving cycle data, as shown in Fig. 3 and Fig. 4, the battery capacity is determined to be 4 kWh. The modelled components of the hybrid drive system will have the following specifications.

Tab. 7. Component specifications of the vehicle

| Component | Specification | Mass |
|--------------|----------------------|-------|
| Engine | Gasoline, Air-cooled | 16kg |
| Generator | 4 kW AC Induction | 20 kg |
| Motor | AC Induction | 50kg |
| Battery Pack | Li-ion | 33kg |
| Vehicle | TVS King | 610kg |

The various power and torque requirements of the vehicle are plotted for various speeds in kmph for the vehicle in the tractive effort curve as shown in Fig. 4. The type of hybrid configuration chosen for the vehicle is simple serial hybrid as shown in Fig. 5, where the traction motor, of AC Induction type is used to directly power the wheels. The downsized Internal Combustion (I.C.) engine is used as an auxiliary power source to power the vehicle during high acceleration requirements and also to maintain the State of Charge (SoC) of the battery pack. This

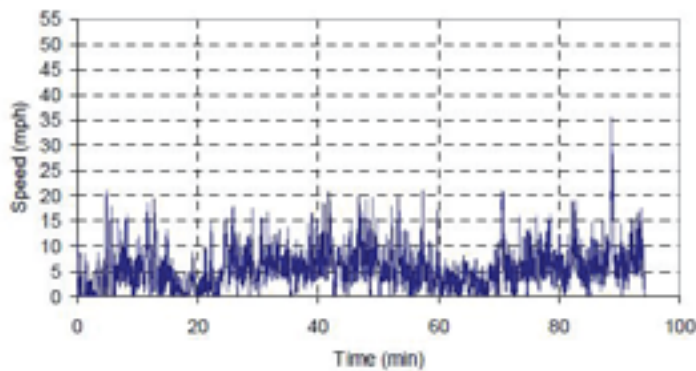


Fig. 2. Daytime driving cycle of auto rickshaw [4]

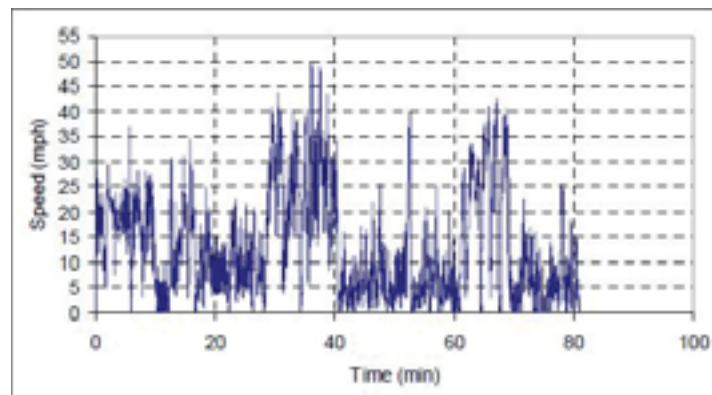


Fig. 3. Evening time driving cycle of the vehicle [4]

type of hybrid architecture is chosen for two primary reasons. First, the drivetrain and controller complexity is reduced. Secondly, the engine is made to operate at its best efficiency point, thereby increasing the fuel economy and minimizing the impact of carbon footprint on the atmosphere.

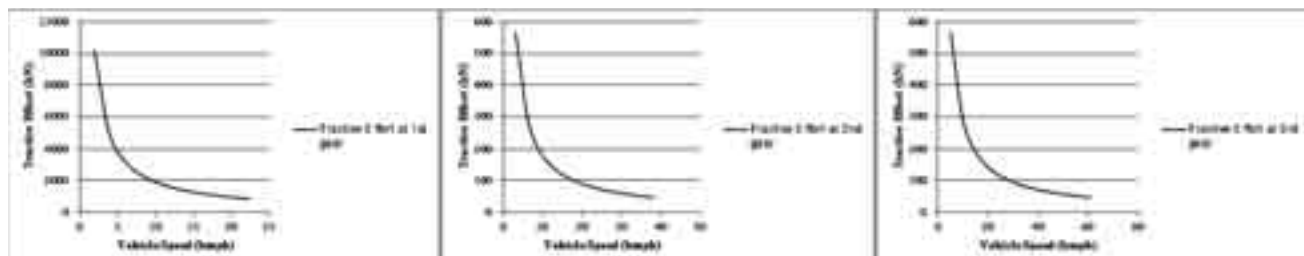


Fig. 4. Tractive effort curve

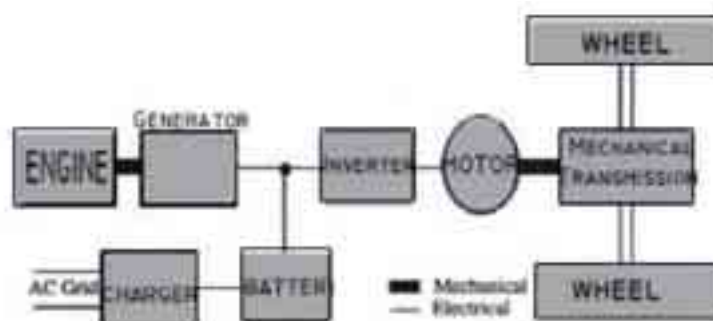


Fig. 5. Hybrid architecture

4. Use of renewable energy technology

With the challenge of rising pollution levels in India, it is estimated that the total energy demand is likely to increase around 1.8 btoe in 2030 from 0.5 btoe in 2005 and the subsequent green house gas (GHG) emissions would increase from roughly 1.6 billion tonnes CO₂eq in 2005 to 5.0 billion to 6.5 billion tonnes CO₂eq in 2030 [5]. Thus, there is a very strong necessity to utilize the cleaner energy sources for maximizing the energy security and environment benefits for the vehicle fleets, which is likely to grow seven fold by 2030. India has a very good solar potential with 300 clear sunny days as it receives very high solar radiation. The considered city of Coimbatore (Tamil Nadu, India 11.0183° N, 76.9725° E) has monthly average solar radiation values ranging from 3.71 to 6.39 kWh/m². The wind power generation capacity is estimated to be 273 W/m² with the wind speed ranging from 12 m/s to 18 m/s in specific potential zones. With such a large potential for non-conventional energy sources, a synergy could be established between the PHEVs and the RET by powering the battery charging stations through efficiently harnessing these natural resources. A brief methodology is adopted to determine the components of the system and sizing of the components. Thus, the expected power generation capacity and the supporting infrastructural facilities required at the considered area are quantified.

4.1. Modelling of the Solar Photo Voltaic System

The major components of the system are Solar Photovoltaic (PV) module, battery storage system, charge controller, auxiliary generator and inverter, if AC output is required. Taking the least value from the calculation for the Levelised Cost of Energy (L.C.E.), the proportion of Solar and wind power harnessing to be done is in the ratio of 30:70 for our study. Thus, the energy demand for solar charging station is 2.4 kWh per day. The following assumptions are made for sizing of PV components, which is of the type Stand Alone System with Battery Storage.

Tab. 8. Assumptions made for the estimation of solar battery charging station

| Parameter | Unit | Value |
|---|--------------------------|-------|
| Solar Irradiance AM1.5 | kW/m ² | 0.97 |
| Average Solar Insolation | kWh/ m ² /day | 3.71 |
| Efficiency = Rated Power/(AM1.5_power_density*Area) | % | 10 |
| Battery charging efficiency | % | 85 |
| Vehicle charging efficiency | % | 90 |
| Inverter efficiency | % | 93 |

$$E_1 = \frac{E_2}{[x n_1 + (1-x)] n_2} P = \frac{E_1 \cdot \text{solar_irradiance}}{\text{Average insolation}}, \quad (3)$$

where:

E_1 – energy rating of the PV,

E_2 – energy demand,

x – proportion of excess energy stored in battery,

n_1 – efficiency of the battery,

n_2 – efficiency of vehicle charging,

P – required rated power.

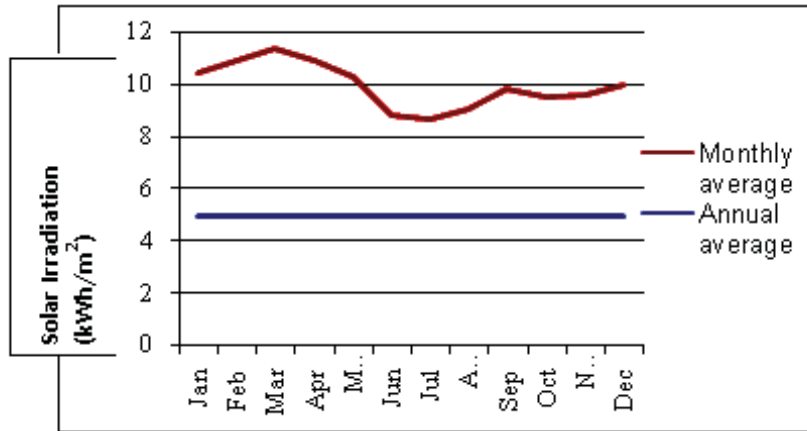


Fig. 6. Monthly GHI of Solar Irradiation at Coimbatore (Tamil Nadu, India) [6]

From the above equations the energy requirement of the PV, E_{PV} and the corresponding rated power P_{rated} is determined as 3.2 kWh and 0.863 kW, respectively. Accounting the efficiency of 10% for Solar PhotoVoltaic (SPV), the rated power at coimbatore charging station is, $P_{rated} = 8.63\text{ kW}$. Amongst the available material technologies polycrystalline material is chosen for PV modules as it has a slightly lower conversion efficiency compared to single crystalline and the manufacturing costs are also lower. The module efficiency averages about 10% to 11%. Based upon the levelized cost of energy (LCoE) calculations and taking in account the maximum area of PV modules for harnessing solar power, 225W (peak power) PV module suits our need with a total area requirement of 0.482m². The electrical characteristics of the chosen SPV module such as Multi Point Power Tracking (MPPT), etc., are given in Tab. 9.

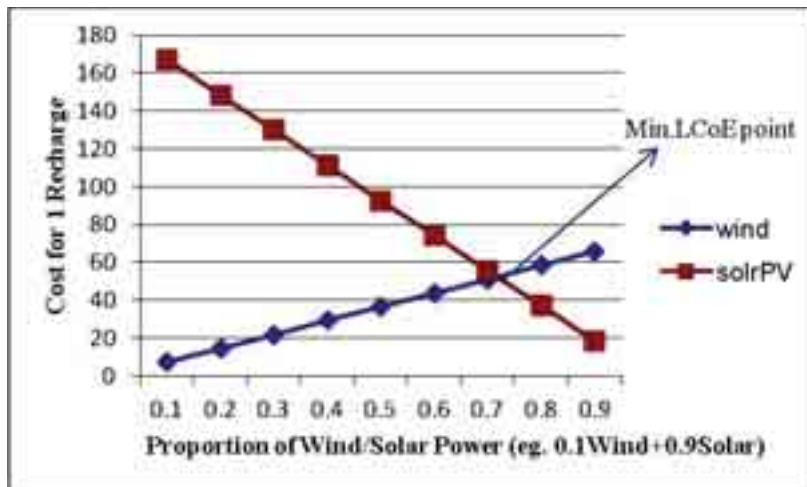


Fig. 7. Graph for LCoE for wind and solar power

Tab. 9. Characteristics of the solar PV system

| Parameter | Value |
|--------------------------|---------|
| Watt at Maximum Power | 225 Wp |
| Open Circuit Voltage | 33.60 V |
| Short Circuit Current | 9.35 A |
| Voltage at Maximum Power | 26.70 V |
| Current at Maximum Power | 8.43 A |
| Maximum System Voltage | 1000 V |
| Series Fuse Rating | 15 A |

The parameter values are defined at an irradiance of 1000 W/m^2 , at coimbatore with AM1.5 Solar Spectrum and temperature 25°C . The month wise generation capacity of SPV and wind energy at Coimbatore locations depicted in Tab. 10.

Tab. 10. Monthwise generation capacity estimation of solar/wind energy at coimbatore city

| Month(kWh/m^2) | January | February | March |
|---------------------------|---------|----------|-----------|
| Generated PV Energy | 5.46 | 5.94 | 6.39 |
| Generated Wind Energy | 1.417 | 0.823 | 1.037 |
| Month(kWh/m^2) | April | May | June |
| Generated PV Energy | 5.93 | 5.35 | 3.87 |
| Generated Wind Energy | 0.950 | 1.612 | 4.745 |
| Month(kWh/m^2) | July | August | September |
| Generated PV Energy | 3.71 | 4.08 | 4.83 |
| Generated Wind Energy | 4.363 | 3.687 | 1.6725 |
| Month(kWh/m^2) | October | November | December |
| Generated PV Energy | 4.54 | 4.65 | 4.99 |
| Generated Wind Energy | 0.786 | 0.933 | 1.950 |

4.2. Modelling of the Wind Energy System

The foremost task in modelling a wind energy system is wind resource estimation, termed as micrositing. The site-specific details of the wind energy stations are as, given in the Tab. 11.

Tab. 11. Site specifications of the wind energy station to be installed [7]

| Parameter | Unit | Value |
|--------------------------------|----------------|-------|
| Average Annual Wind Speed | m/s | 3.36 |
| Elevation | masl | 444 |
| Mean annual wind power density | W/m^2 | 273 |

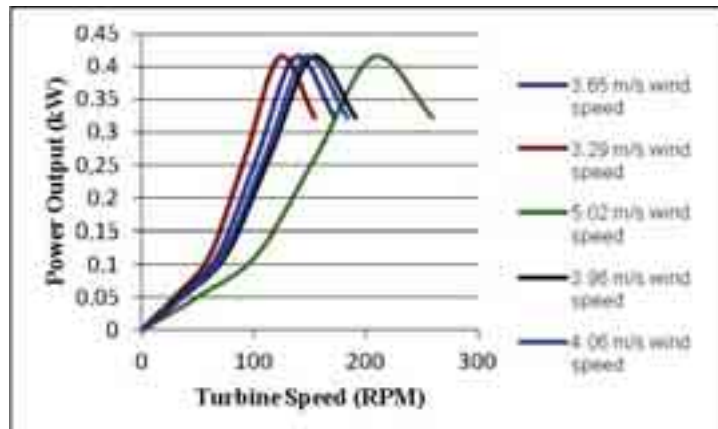


Fig. 8. Wind turbine characteristic curve

The power generated from the turbine is calculated using various wind parameters given in equation (4)

$$P = 0.5 \rho A C_p v^3 \eta_g \eta_b , \quad (4)$$

where:

- P – power (W),
- ρ – density (kg/m^3),
- A – swept area (m^2),

- C_p – power coefficient,
 v – wind speed (m/s),
 η_g – efficiency of generator (%),
 η_b – efficiency of gearbox bearing (%).

The various power output for different wind speeds at the chosen location is plotted in Fig. 10. The turbine is sized to charge three sets of battery packs for the vehicle. The major components of this system are Wind Turbine Generator (WTG), Voltage Control System (VCS) / DC-DC System, battery storage and an auxiliary generator. The components sizing are done based on the LCoE. Thus, based on the lowest value for the LCoE the components if the system is sized as follows:

Tab. 12. Component specifications of the wind energy charging station

| Component | Specification |
|------------------------|--------------------|
| Wind Turbine Generator | 1 kW |
| Cut in Wind Speed | 3m/s |
| Cut out Wind Speed | 30 m/s |
| Rated RPM | 180 RPM |
| Swept area | 3.24m ² |

5. Charging methodology

Most Lithium ion battery chargers that are in use today use the so-called CC/CV characteristics, where a constant current (CC) is used for the main charge and a constant voltage (CV), for the final charge. The duration of the main charge phase depends on the charge current, whereas the final charge, which only needs a small current, does not depend on it [8]. In this study, the charging capabilities of the different batteries for the main charging phase (CC) have been analyzed based on charging rates from 1/3C to 3C for LFP, NMC, NCA and NMS. The results in Fig. 9 indicate that the NiCoMnO₂ (NMC) and NiCoAlO₂ (NCA) chemistry types are most suited for fast charging. The charging capacity up to V_{max} is around 88% of the mentioned manufacturer capacity. However, the batteries using iron phosphate or manganese oxide in the positive electrode have comparatively lesser capacity characteristics at higher charging rates. Further, the energy efficiency at different C-rates has been investigated. To be suitable for BEV and PHEV applications the charge efficiency of the battery should be 90% to 95%. This aspect can be considered as most important in PHEV applications due to the fact that the losses due to the build-up of internal resistance will cause the temperature of the battery to rise. Due to this reason, at current rates higher than 1C the charge efficiency of all the battery chemistries (NMC, NCA, LFP, and MNS) is almost less than 90%. Thus for better energy efficiency a current rate of 1C is chosen.

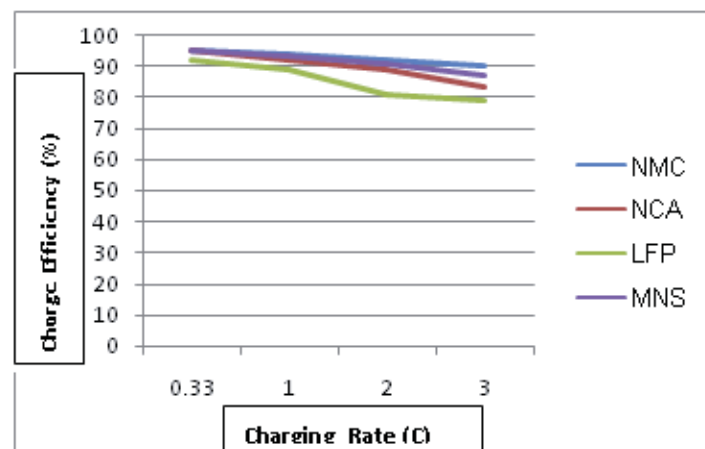


Fig. 9. Charge capacity (C) at different charging rates [9]

Life cycle of a battery can be also considered as a keyparameter for charging rate determination. By the Electric Power Research Institute (EPRI) standards, the battery should be able to perform 1400 cycles during the charge-depleting phase (80% DoD).The simplest way for predicting battery longevity is Peukert's equation, as stated in equation (5). Assuming charging and discharging cycles as per the ISO 12405-2 the percentage change in life cycle for all the battery chemistries are analyzed. The comparison shows that the life cycle of LFP battery chemistry is much higher at 40°C than NCA, NMC and MNS [10]

$$I t = C \left(\frac{C}{I H} \right)^{k-1}, \quad (5)$$

where:

- t – discharge time (h),
- I – discharge current (A),
- H – rated discharge time (h),
- C – rated capacity at that discharge rate (Ah),
- k – Peukert constant (dimensionless).

Iron phosphate based and NMC based technology possesses superior thermal and chemical stability, which provides better safety characteristics than those of lithium-ion technology made with other cathode materials [11].

6. Conclusion

1. With the use of renewable energy sources for the propulsion of this widely used public transit vehicles, there would be a significant decrease in GHG emission and thus have a corresponding effect on the Global Warming Potential (GWP), as well.
2. Analysing the different lithium chemistry, which is suitable, lithium MNC, was chosen to be the potential candidate for PHEV propulsion in terms of high energy density, moderate power density and cost.
3. The thermal safety of the battery is maintained by management of the heat released by using passive thermal management systems, which proved to be very beneficial for such lightweight demanding applications.
4. Safe and relatively fast charging the battery packs as compared to the conventional charging, with maintaining the battery cycle life has been quantitatively done

References

- [1] Greg Albright, Jake Edie, Said Al-Hallaj, *A Comparison of Lead Acid to Lithium-ion in Stationary Storage Applications*, Published by AllCell Technologies LLC, March 2012.
- [2] Omar, N., et.al., *Assessment of Performance of Lithium Iron Phosphate Oxide, Nickel Manganese Cobalt Oxide and Nickel Cobalt Aluminum Oxide Based cells for Using in Plug-in Battery Electric Vehicles*, Proceedings of the Vehicle Power and Propulsion Conference, pp. 1-7, Chicago IL 2011.
- [3] Heinz, A., et al., *Application of Phase Change Materials and PCM-Slurries for Thermal Energy Storage*, Proceedings of the ECOSTOC Conference, Session 12B – Transportation of Energy, New Jersey 2006.
- [4] Lukic, Srdjan M., et.al. *Usage Pattern Development for Three-Wheel Auto rickshaw Taxis in India*, Proceedings of the Vehicle Power and Propulsion Conference, pp. 610-616, Arlington TX 2007.
- [5] Meisen, P., *Overview of Renewable Energy Potential for India*, Global Energy Network Institute, 2006.

- [6] SynergyEnviroEngineers, http://synergyenviron.com/tools/wind_data.asp?loc=Coimbatore%2CTamil%20Nadu%2CIndia.htm, retrieved on 24 April 2012.
- [7] Sreevalsan, E, et.al., *Indian Wind Atlas*, Centre for Wind Energy Technology, pp. 139, 2010.
- [8] Omar, N., et.al., *Power and life enhancement of battery-electrical double layer capacitor for hybrid electric and charge-depleting plug-in vehicle applications*, Journal of the International Society of Electrochemistry, 2010.
- [9] Omar Noshin, et.al., *Evaluation of performance characteristics of various lithium-ion batteries for use in BEV application*, 2010.
- [10] Omar, N, et.al., *Assessment of Performance of Lithium Iron Phosphate Oxide, Nickel Manganese Cobalt Oxide and Nickel Cobalt Aluminum Oxide Based cells for Using in Plug-in Battery Electric Vehicle Applications*, 2011.
- [11] Nelson, P, Bloom, I., Amine, K., Henrikson, G., *Design modelling of lithium-ion battery performance*, Journal of Power Sources, Vol. 100, pp. 437-444, 2002.